Covariation of vegetation and climate constrains present and future T/ET variability

Environmental Research Letters

LETTER

Covariation of vegetation and climate constrains present and future T/ET variability

Athanasios Paschalis[1], **Simone Fatichi**[2], **Christoforos Pappas**[3,4] **and Dani Or**[5]

[1] Department of Civil and Environmental Engineering, Imperial College London, United Kingdom
[2] Institute of Environmental Engineering, ETH Zurich, Switzerland
[3] Département de Géographie and Centre d'Études Nordiques, Université de Montréal, Montréal, QC, Canada
[4] Faculty of Environmental Sciences, Czech University of Life Sciences Prague, Czechia
[5] Department of Environmental Systems Science, ETH Zurich, Switzerland

E-mail: a.paschalis@imperial.ac.uk

Keywords: T/ET, evapotranspiration partitioning, ecohydrology, modelling, climate change

Supplementary material for this article is available online

OPEN ACCESS

RECEIVED
30 April 2018

REVISED
17 September 2018

ACCEPTED FOR PUBLICATION
19 September 2018

PUBLISHED
5 October 2018

Abstract

The reliable partitioning of the terrestrial latent heat flux into evaporation (E) and transpiration (T) is important for linking carbon and water cycles and for better understanding ecosystem functioning at local, regional and global scales. Previous research revealed that the transpiration-to-evapotranspiration ratio (T/ET) is well constrained across ecosystems and is nearly independent of vegetation characteristics and climate. Here we investigated the reasons for such a global constancy in present-day T/ET by jointly analysing observations and process-based model simulations. Using this framework, we also quantified how the ratio T/ET could be influenced by changing climate. For present conditions, we found that the various components of land surface evaporation (bare soil evaporation, below canopy soil evaporation, evaporation from interception), and their respective ratios to plant transpiration, depend largely on local climate and equilibrium vegetation properties. The systematic covariation between local vegetation characteristics and climate, resulted in a globally constrained value of T/ET $= \sim 70 \pm 9\%$ for undisturbed ecosystems, nearly independent of specific climate and vegetation attributes. Moreover, changes in precipitation amounts and patterns, increasing air temperatures, atmospheric CO_2 concentration, and specific leaf area (the ratio of leaf area per leaf mass) was found to affect T/ET in various manners. However, even extreme changes in the aforementioned factors did not significantly modify T/ET.

1. Introduction

Evapotranspiration is among the largest land fluxes of water accounting for ~60% of terrestrial precipitation at the global scale (Oki and Kanae 2006, Katul *et al* 2012). It is also an energy demanding process, accounting for the largest fraction of the total net terrestrial radiation (Wang and Dickinson 2012, Wild *et al* 2015, Fatichi *et al* 2016b). For this reason, latent heat fluxes, particularly at the land surface, play a major role for weather dynamics including the development of mesoscale systems (Houze 2004), triggering convection and initiation of rainfall (Seneviratne *et al* 2010, Gentine *et al* 2013, Manoli *et al* 2016) and persistence of heat waves (Fischer *et al* 2007, Lorenz *et al* 2010). Predictive understanding of evapotranspiration dynamics as a part of the coupled Earth system is essential, due to their potential impacts on global food security (Schmidhuber and Tubiello 2007), water resources (Oki and Kanae 2006) and economy (Mendelsohn *et al* 2000).

The partitioning of latent heat flux (ET) into its biotic (T; transpiration) and abiotic (E; soil evaporation and evaporation of canopy interception) components is of major importance. Plant transpiration is inherently linked to vegetation dynamics through leaf area and stomatal conductance and its impacts on photosynthesis. At the same time, stomatal conductance is linked to environmental forcing (e.g., air temperature, vapour pressure deficit (VPD),

atmospheric CO_2 concentration) and to the root-zone soil water availability (Keenan *et al* 2010, Buckley and Mott 2013, Fatichi *et al* 2016a). Abiotic evaporation depends also on (i) meteorological variables regulating the atmospheric water demand and (ii) vegetation structural properties, such as leaf area and canopy structure, that could modify the energy balance at the land surface (e.g., through shading) and determines the area available for intercepting rainfall.

Despite the importance of ET partitioning, global-scale estimates commonly diverge. Observational studies have reported values of the transpiration-to-evapotranspiration ratio (T/ET) spanning a wide range of values globally, from ~60% ± 25%; (Coenders-Gerrits *et al* 2014) up to ~85% ± 5%; (Jasechko *et al* 2013) with several recent studies reporting different estimates (Coenders-Gerrits *et al* 2014, Wang *et al* 2014, Good *et al* 2015, Berkelhammer *et al* 2016, Zhou *et al* 2016, Wei *et al* 2017). T/ET in boreal peatland ecosystems has been also found to be as low as 1% (Warren *et al* 2018). Most observational-based estimates were derived using either water isotope data (Jasechko *et al* 2013) or eddy-covariance flux tower data (Zhou *et al* 2016). T/ET estimates in both approaches are indirect and sensitive to flux partitioning assumptions and measurement errors (see Fatichi and Pappas (2017) and Berkelhammer *et al* (2016)).

Modelling studies have shed additional light in the quantification of T/ET. Simplified modelling approaches based on variants of the Penman–Monteith equation have provided estimates of T/ET close to the observational range (Choudhury and DiGirolamo 1998, Zhang *et al* 2016). However, these approaches do not take into account the coupled behaviour of the water and carbon cycles, since vegetation properties are often prescribed, and thus their predictive skill for future climatic conditions is limited. Detailed ecosystem models that resolve simultaneously water, energy and carbon dynamics at the land surface using physical principles offer a mechanistic interpretation of the T/ET variability. Recently Fatichi and Pappas (2017) used such a modelling approach to estimate the distribution of T/ET across a large number of sites. They found the T/ET ratio to be constrained around ~70%, within the observational range, and almost independent of climate and vegetation properties. This challenges previous findings that ascribed various controls over T/ET variability across ecosystems, such as leaf area index (LAI) and stomatal conductance (Cavanaugh *et al* 2011, Wang *et al* 2014, Wei *et al* 2017).

Despite the large number of studies estimating T/ET, a clear mechanistic explanation of its global distribution is lacking. Investigating the underlying mechanisms that limit T/ET frame the scope of this study. We hypothesize two district patterns of T/ET responses to vegetation structural properties at dry and wet climates, illustrated in figure 1. In a dry climate, i.e., arid ecosystems, we hypothesize that, T/ET is limited due to the sparse vegetation cover (reflecting long-term water availability) where an upfront surface evaporation loss occurs before any of the precipitation water becomes available for T. More specifically, in arid ecosystems, ET is expected to be roughly equal to precipitation and only the fraction of water that is not rapidly lost through surface evaporation after rainfall becomes useful for transpiration, thus limiting the T/ET value. This upfront cost is expected to be non-negligible since even in an ideal situation for the plants, where drip irrigation was used, evaporation has been found to be at least ~10% of ET (see review from Kool *et al* (2014)). While a higher vegetation cover could potentially use more water through transpiration, such an increase in vegetation biomass is not sustainable in the long-term due to limited water availability. At the same time, plants in dry climates have adapted conservative strategies for efficient use of the limited water. This behaviour leads to a steep rise of T/ET as a function of leaf area (figure 1(a)). This rise will taper off with increased leaf area where additional increase in the transpiring area will induce stronger soil water stress. Considering optimality arguments that postulate maximization of water use without substantially increasing water stress (Caylor *et al* 2009, Manzoni *et al* 2014), we hypothesize that leaf area in undisturbed arid ecosystems should have values that maximize T/ET. In wet climates where available energy becomes limiting (e.g. tropical forests) ET is roughly equal to potential ET. In these ecosystems, we hypothesize that LAI is also nearly optimal and maximizes T/ET (figure 1(b)). An increase in LAI in comparison to current values would lead to more evaporative losses due to interception and thus reduce T, since total ET is energy constrained. A reduction of LAI would also reduce T due to reduced area for transpiration. Combining these two arguments, we hypothesize that for ecosystems in the range between water and energy limited conditions, T/ET spans a constrained range defined by these two end members of the wetness-energy spectrum.

The aforementioned hypotheses are tested by analysing statistical dependences among observed climate and vegetation variables driving ET and its component (e.g., precipitation, LAI). We further ask if T/ET is expected to change under future climatic conditions. To answer this question and test the hypotheses put forward, we expand upon the results of Fatichi and Pappas (2017). In summary, we seek (a) a mechanistic explanation of the apparent global constancy of T/ET ratio and (b) a quantification of the potential impacts of climate change on the partitioning of evapotranspiration components.

2. Methods

For the statistical analysis of the variability in T/ET, three sets of simulations were conducted. The first was

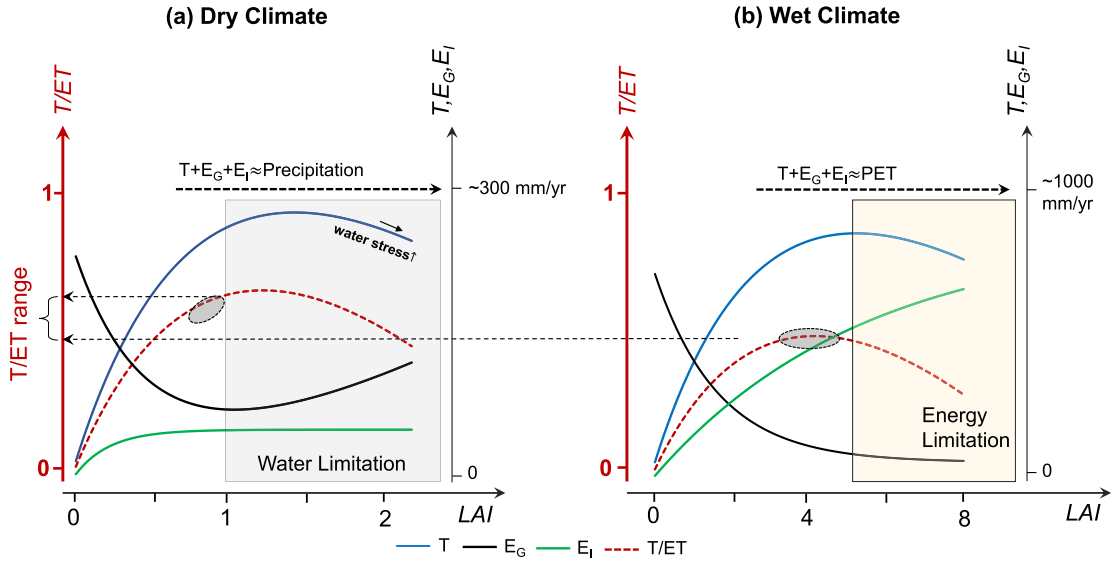

Figure 1. Schematic representation of the study's hypotheses for the relation between transpiration (T), soil evaporation (E_G), evaporation from interception (E_I), ratio of transpiration of (T/ET) and leaf area index (LAI), for dry (a) and wet (b) climates. Shaded areas in panel (a) correspond to inaccessible values of LAI due to limited water availability. Shaded areas in panel (b) correspond to inaccessible values of LAI due to energy (light or temperature) limitations. Dark grey shaded areas indicate typical values of LAI in equilibrium with the local climate.

derived from the study reported in Fatichi and Pappas (2017) and describes current vegetation in equilibrium with present climate. The second was a sensitivity analysis of T/ET against variability in rainfall structure and LAI, and the third set of simulations investigated the variability of T/ET under future climatic conditions. For all three simulations, the model parameters were kept the same, and for each site used in this study, model parameterization was identical to Fatichi and Pappas (2017). A detailed parameter sensitivity analysis in Fatichi and Pappas (2017) excluded the possibility that parameter uncertainty can significantly influence the estimates of T/ET.

2.1. Present climate-modelling and statistical analysis

The statistical analyses for the present climate are based on the model simulation results reported in Fatichi and Pappas (2017). Seventy nine sites spanning diverse climates and biomes, representative of most regions in the world (supporting material—figure S1 is available online at stacks.iop.org/ERL/13/104012/mmedia), were simulated using the T&C ecohydrological model (Fatichi *et al* 2012a, 2016a, Paschalis *et al* 2015, 2016, Manoli *et al* 2018). The model simulates the coupled energy, water and carbon cycles using mechanistic formulations. Vegetation is dynamic with leaf and root biomass being prognostic variables allowing for explicit simulation of the effects of climate change in the ecohydrological responses (e.g. terrestrial carbon, water and energy fluxes). Evapotranspiration and its components are simulated explicitly by solving the energy balance at the land surface, without adopting common empirical simplifications often used in hydrology. The water and carbon cycles are linked through leaf stomatal conductance using the widely used Leuning model (see Paschalis *et al* (2016) for a more detailed discussion). However, as most land surface models, T&C does not resolve explicitly the effect of small scale micrometeorological heterogeneity that can influence water fluxes, such as lateral heat fluxes in patchy or disturbed sites including forest edge effects. Model details can be found in Fatichi *et al* (2012a, 2012b) and Mastrotheodoros *et al* (2017). Using the model simulation results we decomposed the ratio of total (integrated hourly simulations for the total simulation period) transpiration (T; mm yr^{-1}) to total evapotranspiration (ET; mm yr^{-1}) as

$$\frac{\mathrm{T}}{\mathrm{ET}} = \frac{\int_{sim-years} \mathrm{T}^{(h)} dt}{\int_{sim-years} \mathrm{ET}^{(h)} dt} \approx \frac{\mathrm{T^g}}{\mathrm{T^g} + \mathrm{E_G^g} + \mathrm{E_G^d} + \mathrm{E_I^g}}. \quad (1)$$

$\mathrm{T}^{(h)}$ and $\mathrm{ET}^{(h)}$ are the hourly modeled values of transpiration and evapotranspiration respectively. $\mathrm{T^g}$ is the transpiration when canopy is present (i.e., LAI $>$ 0). Ground evaporation was sub-divided into $\mathrm{E_G^g}$ and $\mathrm{E_G^d}$, corresponding to two different time periods. The former, $\mathrm{E_G^g}$, refers to the time when LAI $>$ 0 and lumps evaporation from shaded areas bellow the canopy and evaporation from bare soils in the case of patchy vegetation that occurs in semi-arid locations. The latter, $\mathrm{E_G^d}$, refers to time periods when canopy is absent, and no shading occurs. $\mathrm{E_I^g}$ is the evaporation from intercepted water on the canopy, occurring only when LAI $>$ 0. $\mathrm{T^g}$ is the biotic component of ET and $\mathrm{E_G^g}$, $\mathrm{E_G^d}$, $\mathrm{E_I^g}$ are the abiotic components. In equation (1), we excluded snow sublimation,

since for most of the sites analysed here is negligible or small. Using this algebraic decomposition, we scrutinized the T/ET dynamics by seeking statistical dependencies between the three ratios E_G^g/T^g, E_G^d/T^g, E_I^g/T^g for each site and various climate and vegetation descriptors. The three ratios correspond to the relative strengths of the three major abiotic components of ET to its sole biotic component. Given that the water and carbon cycles are coupled through highly nonlinear dynamics, we did not aim to unravel the causal structure between water fluxes and vegetation properties, but rather to quantify their statistical correlation structure.

T^g depends on atmospheric demand (i.e. VPD), available solar energy, total transpiring area, stomatal conductance and water stress induced by soil water availability. Atmospheric demand (dependent on air temperature and relative humidity) and solar energy are simultaneously described by potential evapotranspiration. Available solar radiation also depends on radiation attenuation through the canopy, which depends on LAI. Transpiring area is directly related to LAI and vapour flux from this area is related to stomatal conductance. Stomatal conductance further depends on various meteorological variables, including VPD and leaf surface temperature (Paschalis *et al* 2017). Leaf surface temperature depends on the fraction of absorbed radiation converted into sensible heat. This fraction can be encapsulated through the evaporative fraction EF. E_G^g, E_G^d, and E_I^g primarily depend on atmospheric demand, available energy either at the ground (E_G^g, E_G^d), or at the canopy (E_I^g) and water availability at the soil surface and in the canopy interception storage. Soil- and canopy-available water can be captured by the statistical properties of precipitation, in particular, its total amount and temporal structure (e.g., the storm frequency). However, given that long-term ET is strictly lower than the total precipitation amount (P_{TOT}), P_{TOT} cannot be used as an independent variable and thus we chose the commonly used wetness index (defined as the ratio of annual precipitation to annual potential evapotranspiration) to describe the effect of the amount of precipitation in the components of ET. Summarizing, on the basis of these considerations, we finally chose the storm arrival rate, $\lambda[h^{-1}]$, leaf area index, LAI $[m^2\,m^{-2}]$, wetness index, WI [-], mean annual air temperature, T_a [°C], and evaporative fraction, EF [-], as explanatory variables that should embed all controls in transpiration and evaporation components (figure 2). We expressed the statistical dependence of the fractions E_G^g/T^g, E_G^d/T^g, E_I^g/T^g to the chosen descriptors using multivariate linear models (supporting information). While λ, WI, T_a, EF are measured meteorological variables that can be directly used as independent explanatory variables, the value of LAI used in this study comes from the model itself, since in most locations *in situ* LAI measurements were not available. However, a very good agreement between simulated LAI and LAI estimates from MODIS ($R^2 = 0.6$, RMSE $= 1.3\ m^2m^{-2}$ for the mean growing season LAI) alleviates the risk of biasing our analysis towards a high dependency on LAI. Furthermore, LAI estimates derived by the model avoid the issue of scale discrepancy between simulations and remote sensing LAI observations, which are at coarse scale ($>1\ km^2$).

2.2. Sensitivity analyses

2.2.1. Sensitivity of T/ET to LAI and λ

For the second set of simulations we performed a sensitivity analysis of T/ET against the most important drivers identified in the previous step (see section 3.1), namely, LAI and λ. For this set of simulations, LAI was not a prognostic variable within T&C, but was prescribed *a priori*. The prescribed LAI was defined as $LAI_p = \alpha * LAI_c$, where LAI_c were the originally simulated LAI time series by the T&C used for maintaining realistic seasonal patterns, and $\alpha[-]$ a multiplier. The storm frequency λ was perturbed by either randomly introducing (λ increase) or removing (λ decrease) storms from the rainfall time series. The selection of the introduced storms was done by sampling with replacement from the set of observed storms while their time of occurrence was randomly selected. The removal of storms was done with random sampling. After the storm structure was perturbed, the intensities were rescaled so that the total amount of rainfall was equal to the observed one. The sensitivity analysis was performed for three different climates: a semi-arid (Vaira Ranch, CA, USA—Ameriflux site US-Var; Baldocchi *et al* (2004)), a temperate (UMBS, MI, USA—Ameriflux site US-UMB; Curtis *et al* (2005) Hardiman *et al* (2011)) and a tropical site (Manaus—Ameriflux site ZF2 K34; Araújo (2002)). Those three sites experience different water and carbon dynamics and encapsulate the dependencies of T/ET on vegetation sparseness and climate wetness, upon which we built our hypotheses. Similar sensitivity analyses were conducted using different stations (not shown here) and the results remained identical. However, for illustrative purposes we present only three representative sites.

We analysed the simulated T/ET by comparing the imposed values of rainfall frequency, expressed as the number of wet days per year, and simulated LAI to observed values at the global scale. As observations we used the number of wet days derived from the CRU 4.10 dataset (Harris *et al* 2014) and LAI derived by the MODIS—GLASS product (Xiao *et al* 2014) (see supporting information for more details).

2.2.2. Sensitivity to climate and vegetation structure

In the second sensitivity analysis we conducted twenty-five (5×5) numerical experiments where: (a) atmospheric CO_2 concentration, (b) air temperature, (c) specific leaf area, Sla, (d) total annual precipitation and (e) frequency of rainfall events were perturbed as

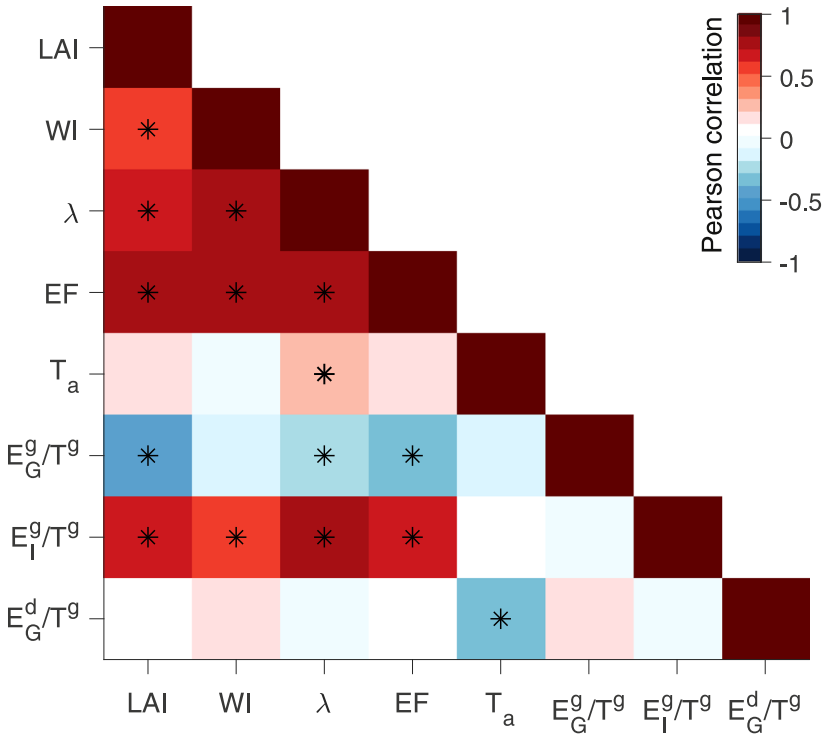

Figure 2. Pearson correlation coefficients between (E_G^g/T^g, E_G^d/T^g, E_I^g/T^g) describing the ratios of ground evaporation in the presence of foliage (E_G^g), evaporation in the absence of foliage (E_G^d) and evaporation from interception (E_I^g) to transpiration (T^g), and their four statistical descriptors, namely, leaf area index (LAI), storm arrival rate (λ), evaporative fraction (EF) and mean annual temperature (T_a). Star signs indicate statistically significant correlations (p-value < 0.1).

Table 1. Description of the examined explanatory variables for T/ET (a–e) and the twenty-five numerical experiments (Ex. 1–Ex. 5).

	Ex. 1	Ex. 2	Ex. 3	Ex. 4	Ex. 5
(a) CO_2	380 + 0 ppm	380 + 50 ppm	380 + 100 ppm	380 + 150 ppm	380 + 200 ppm
(b) Air temperature	+0°C	+1 °C	+2 °C	+3 °C	+4 °C
(c) Specific leaf area	−50%	−25%	No change	+25%	+50%
(d) Precipitation amount	−50%	−25%	No change	+25%	+50%
(e) Event frequency	−50%	−25%	No change	+25%	+50%

shown in table 1. Simulations were carried out for all 79 locations.

Those simulations can be thought as proxies of future climates where air temperature and atmospheric CO_2 are expected to be higher, according to all current climate projections (Knutti and Sedláček 2012). Current climate projections are uncertain regarding changes in the amount of precipitation, as well as the change in its temporal structure. Thus, we included simulations where the total rainfall amount and the frequency of precipitation were both increased and decreased. Changes in vegetation structure was simulated considering a change in Sla, a key plant trait (Reich *et al* 1998, Poorter *et al* 2009) that affects simulated vegetation carbon and water dynamics (Pappas *et al* 2016). Air temperature and CO_2 changes were implemented as additive changes, whereas precipitation amount and frequency as well as changes in Sla were multiplicative (table 1). Changes in the precipitation frequency were simulated as described in section 2.2.1.

3. Results and discussion

3.1. Present climate simulations

E_G^g/T^g was negatively correlated with LAI, λ and EF and its correlation to WI and T_a was not statistically significant (p-value < 0.1) (figure 2). Negative correlation implies that an increase of LAI, λ and EF results to a decrease in E_G^g/T^g (supporting information figure S3, table S1).

An increase in LAI shaded the understory and reduced turbulence, decreasing the available energy in the soil and thus reducing soil evaporation. Higher leaf area also increased the interception capacity of the canopy, leading to lower water availability at the ground. In addition, higher values of leaf (transpiring) area increased the total transpiration flux. Those three reasons explained the negative correlation of E_G^g/T^g and LAI.

E_G^g/T^g was also negatively correlated with the storm arrival rate λ (high storm arrival rate implies more frequent rainfalls). Higher storm arrival rates

with the same total rainfall amount were related to weather characteristics that led to frequent, low intensity rain events. This typically results in an increase in rainfall interception loss and less water available at the ground (Gash 1979). Finally, E_G^g/T^g was also negatively correlated to EF This behaviour can be explained by the fact that when the largest fraction of the absorbed radiation is converted to latent heat, it has to follow the most efficient path, that is commonly plant transpiration.

E_I^g/T^g was positively correlated to all statistical descriptors except T_a. Positive correlation between E_I^g/T^g and LAI can be explained by the higher interception capacity of the canopy. The correlation between E_I^g/T^g and WI can be explained by the large amount of water on wet canopies that simultaneously enhances evaporation and hampers transpiration due to its blockage of the leaf stomates. E_I^g/T^g was also positively correlated with λ. This is due to the fact that the amount of intercepted water depends on the number of rainfall events and thus storm frequency (Gash 1979). Finally, E_I^g/T^g was positively correlated with EF because of the higher energy spent in evaporation.

E_G^d/T^g is independent of all descriptors except T_a. The positive correlation between those two variables can be linked to the increased evaporative demand with increasing atmospheric temperature in winter periods without vegetation cover. Given that E_G^d is commonly a small fraction of ET, we will not consider T_a as a relevant statistical descriptor (see supporting information).

Given that all three components of T/ET are dependent on LAI, WI, EF, λ the key question remains, i.e., why T/ET appears to be well constrained across biomes and climatic regions (Schlesinger and Jasechko 2014, Fatichi and Pappas 2017). This remarkable constancy seems to stem from the strong correlation between the climate and vegetation descriptors used in this study (figure 2; table S1; figure S3). Specifically, in geographic regions where precipitation is abundant (high WI), precipitation events are also frequent (high λ) and canopies are thick (high LAI) (figure 2). This results in the concurrent increase of E_I^g/T^g with a decrease of E_G^g/T^g leaving T/ET ratio relatively constant. The opposite occurs in semi-arid regions. Overall, the magnitudes of the various dependencies, expressed quantitatively in the generalized linear model (supporting information) as the model coefficients, are such that they lead to the compensatory behaviour between the three ratios E_G^g/T^g, E_G^d/T^g, E_I^g/T^g. In other words, the current vegetation cover, adapted to the local climate, leads to stable value of T/ET ($70 \pm 9\%$;1.1% standard error of the mean value). Deviations from the current adapted vegetation cover, e.g. through introduction of untenable species, conversion of forests to agricultural land, vegetation degradation through grazing or logging, or changes in climate without the simultaneous modification of vegetation characteristics (i.e. non-adapted vegetation) can modify T/ET.

3.2. Sensitivity analysis

The sensitivity analysis of T/ET to LAI and λ presented in section 2.2.1 strongly supports the argument that vegetation adapted to the prevailing local climate leads to a constrained value of T/ET. Non-adapted vegetation is approximated in this study by prescribing values of LAI. Simultaneous changes in storm arrival rate were imposed in order to capture the co-dependence of T/ET on LAI and λ. LAI and λ were chosen as the two most important statistical descriptors with the highest correlations to the three analysed ratios (figure 2).

For all three locations studied in this sensitivity analysis (figure 3, contour lines), site-level T/ET is highly dependent on both LAI and λ. Specifically, T/ET systematically increases with LAI in the 1–4.5 range and decreases with precipitation frequency and thus the number of wet days per year. The reason of the constancy of T/ET is due to the joint distribution of observed LAI and number of wet days globally. The density of this probability distribution derived by the CRU 4.10 and the GLASS datasets is shown in figure 3 as the background colours. More specifically, in dry areas the number of rainy days and the leaf area are both small (lower left part of figure 3). For this climate regime, the observed joint distribution between LAI and number of observed days has its peak along the contour line of $T \approx 0.7$–0.75, derived using as an example the grassland site in Vaira Rarch. For temperate climates, we chose the deciduous forest at the UMBS as a representative example. For those climates (middle part of figure 3), the observed joint distribution of LAI-number of wet days has its peak aligned with the contour line of T/ET ≈ 0.7. Finally, for warmer, wetter areas with thick canopies, we chose as representative example the tropical forest near Manaus (Brazil). In this case (upper right part of figure 3), the observed joint distribution of LAI-number of wet days has its peak aligned with the contour line of T/ET ≈ 0.7–0.65. As we move from dry to wetter areas WI increases, and T/ET drops from ~0.75 to ~0.65. From this analysis, we also recover the weak negative correlation between T/ET and WI (Fatichi and Pappas 2017). The choice of presenting here these particular three study sites had no bearing on the results, since the analysis was repeated using different sites from the 79 presented in this study (not shown here) with practically identical results.

When vegetation is not adapted to prevailing climate (as during land use transitions or for agricultural crops) the resulting T/ET values may reside outside the current constrained global range of T/ET $= 70 \pm 9\%$ (figure 3). Therefore, it is important to quantify how T/ET could vary due to the

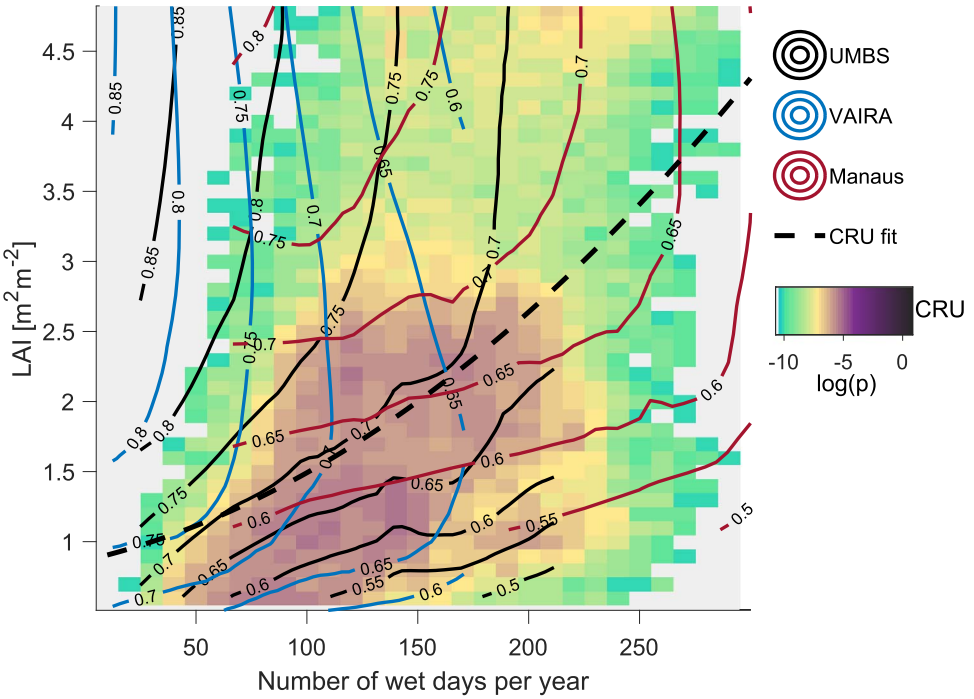

Figure 3. Dependence of T/ET on LAI and the number of wet days per year. Contours represent isolines of constant T/ET derived from model simulations. Black solid lines correspond to the simulations for the UMBS site (Ameriflux US-UMB). Blue solid lines correspond to the simulations of the Vaira Ranch site (Ameriflux—US-Var), and red solid lines to the tropical forest near Manaus Brazil (Aremriflux—Br-Ma2). Background colours indicate the logarithm of the probability density of the joint distribution of LAI and the number of wet days derived from the gridded product CRU 4.01 (Climate Research Unit—University of East Anglia) and the gridded leaf area index estimates from MODIS—GLASS (Global Land Surface Satellite). The black dashed line corresponds to a power law least square fit of the observed CRU-GLASS data.

expected changes in future climate. To evaluate the resilience of T/ET to future climate perturbations, we conducted an additional sensitivity analysis (figure 4). The results of this sensitivity analysis are presented in terms of the fractions of total transpiration, T, evaporation from interception, E_I and evaporation from the ground, E_G with respect to total evapotranspiration, ET for every site.

An increase in the concentration of atmospheric CO_2, leads to a statistically significant but overall small decrease of T/ET and an increase of E_I/ET, despite considerable changes in the total amount of ET (Fatichi *et al* 2016a). The reason for the T/ET reduction is the simulated stomatal closure resulting in reduced transpiration flux not compensated by an overall increase in LAI (Fatichi *et al* 2016a, Paschalis *et al* 2017). E_I/ET increases due to the predicted increase in LAI, because of the CO_2 fertilization effect. The impact of the CO_2 level is stronger in wet regions (supporting information—figure S5). A decrease in Sla, representing canopies with thicker and smaller leaves, can reduce T/ET and E_I/ET, and simultaneously increase E_G/ET. The reason is the decrease in LAI (low Sla values), which reduces the transpiring area, canopy interception capacity, and increases light penetration through the foliage. An increase in Sla does not lead to significant changes in the T/ET ratio indicating a saturation effect at large LAI. Indeed, sensitivity to Sla is stronger at dry places with small LAI (supporting information—figure S5). An increase in the amount of precipitation leads to a small reduction of T/ET, despite the large increases of ET in water limited ecosystems, in agreement with previous findings (Fatichi and Pappas 2017). No statistically significant changes were simulated for E_I/ET or E_G/ET. Sensitivity of T/ET to the amount of precipitation was stronger for dry climates (WI $<$ 1; supporting information—figure S5). Finally, an increase in precipitation frequency can lead to a statistically significant decrease in T/ET and increase in E_I/ET. A decrease of precipitation frequency has the opposite effect. E_G/ET is rather independent of the precipitation frequency in this sensitivity analysis. The sensitivity of T/ET to the precipitation frequency is much stronger when LAI is large (supporting information—figure S5). Large LAI values occur in wet areas where ET is not limited by the total amount of water, and thus the precipitation frequency has the potential to alter the total amount of ET. Temperature increase has no effect on T/ET, E_I/ET or E_G/ET, even though the amount of the respective fluxes is altered the ratios are not. Remarkably, despite the very large changes in climate and Sla prescribed in this sensitivity analysis, the resulting T/ET range is not far from 0.7 ± 0.1 (figure 4).

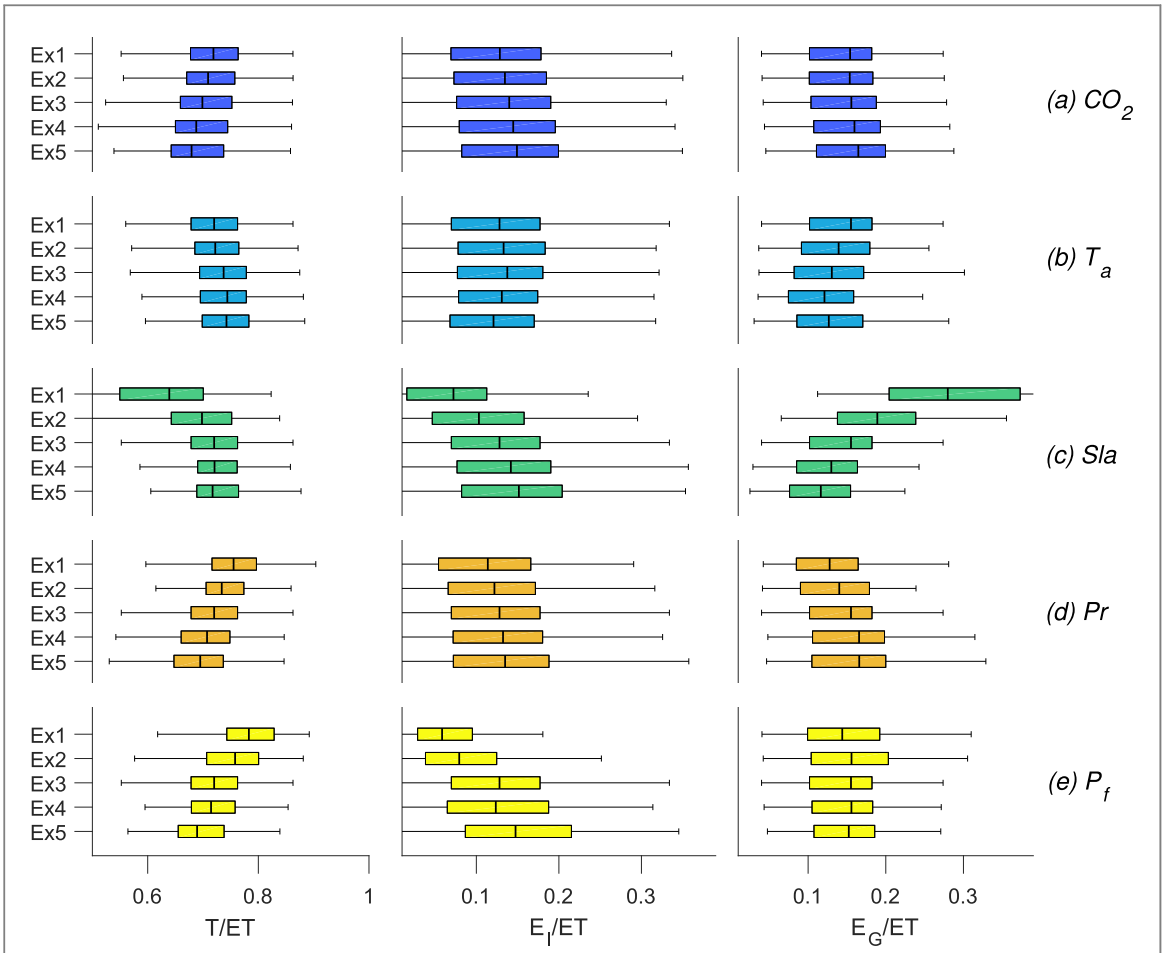

Figure 4. Simulation results for the response of ET components to perturbations in climatic conditions. Boxplots of T_I/ET (first column), (second column) and E_G/ET (third column) for all 25 simulation scenarios. Boxes present the 25%–75% interquartile range and the whiskers the minimum and maximum values. The different rows correspond to experiments with manipulation of (a) atmospheric CO_2; (b) air temperature (T_a); (c) specific leaf area (Sla); (d) total precipitation (Pr); and (e) precipitation frequency (P_f). Details of the experiments are provided in table 1.

3.3. Comparison of T/ET with estimates in previous studies

The analysis presented in sections 3.1 and 3.2 revealed that T/ET (1) is constrained globally with a median value of T/ET $\sim$ 0.7; (2) it is relatively insensitive to future climate changes and (3) its constant global value is attributed to the covariation of precipitation frequency and LAI. However, such constant value occurs only when vegetation and climate are in equilibrium (i.e. adapted vegetation). Alteration in species composition for example through land use changes (e.g. conversion of natural forests to agricultural crops), or changes in the water regimes (e.g. irrigation schemes) can lead to significantly different values of T/ET, potentially outside the convergent range of 0.7 ± 0.09 reported here (figure 3). This could explain why our results differ from various observational-based studies. For example, Wang *et al* (2014) conducted a meta-analysis of previously published T/ET values from 48 studies worldwide and found LAI to be the most important factor determining T/ET (figure 5). Many of the reported sites in Wang *et al* (2014) were agricultural, in which crops do not represent vegetation in equilibrium with the local climate, and may differ considerably from natural vegetation. Consequently, vegetation composition and LAI can be significantly different from what would be naturally expected and is often sustained through irrigation and fertilization. Using the results of the sensitivity analysis presented in section 2.2.1, expanded also for subtropical (US-Dk3—Loblolly pine plantation; Mccarthy *et al* (2007)), boreal (Hyyyalla—Fluxnet ID: FI-Hyy—Evergreen boreal forest; Suni *et al* (2003)) and semi-arid sites (Lucky Hills: Ameriflux ID: US-Whs, semi-arid shrubland; Scott *et al* (2015)), where we set LAI to prescribed values, we could retrieve patterns similar to those reported in Wang *et al* (2014) for LAI > 1 (figure 5(a)). When we exclusively consider sites with natural vegetation from the study of Wang *et al* (2014) (figure 5(b)) the range of the reported values between our study and the meta-analysis is in overall good

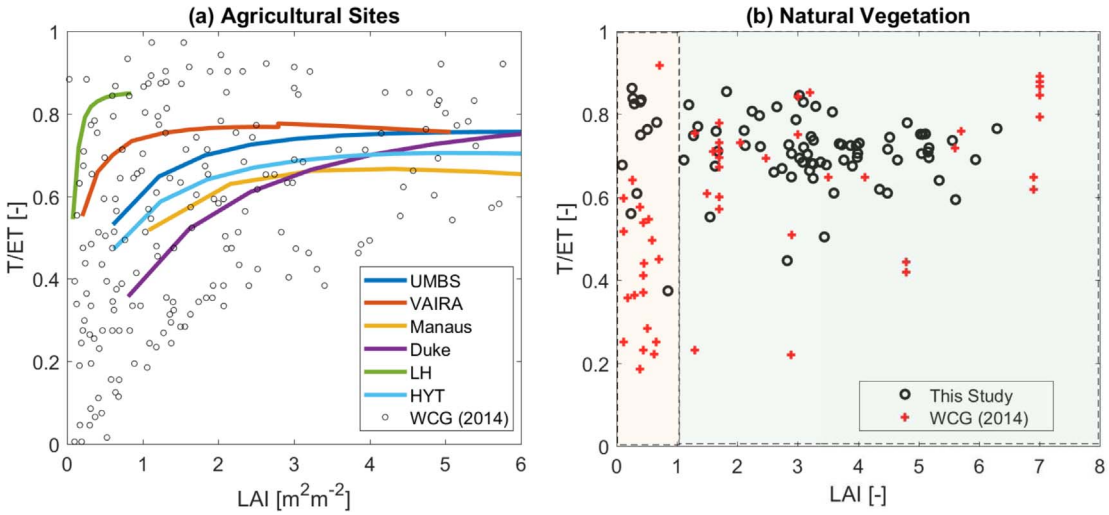

Figure 5. Comparison of the simulation results of the present study with the data from (Wang *et al* 2014—abbreviated as WCG (2014) in the figure). (a) Scatterplot of T/ET versus LAI reported in Wang *et al* (2014) only for agricultural sites (black dots). Lines correspond to simulations for six different sites where LAI was prescribed as an input (*UMBS: Ameriflux ID: US-UMB—deciduous forest; VAIRA: Ameriflux ID: US-Var—grassland; Manaus—Ameriflux ID: Br-Ma2—Tropical forest; Duke: Ameriflux ID:US-Dk3—Loblolly pine plantation; LH: Ameriflux ID: US-Whs, semi-arid shrubland; HYT: Hyyyalla—Fluxnet ID: FI-Hyy—Evergreen boreal forest*). (b) Scatterplot of T/ET versus LAI reported in Wang *et al* (2014) only for sites with natural vegetation (red crosses) together with our simulation results with T&C for the 79 analysed locations (black dots). Data points from Wang *et al* (2014) were extracted using WebPlotDigitizer.

agreement for all sites where LAI $>$ 1. For those sites, the results of Wang *et al* (2014) show a negligible dependence of T/ET on LAI for LAI $>$ 1 with a mean value similar to our results, but larger variability. Larger variability could be attributed to the duration of the measurements, which is typically shorter than our simulations. Site-level T/ET exerts interannual variability that is comparable to the variability among sites (figure S7). This result suggests that part of the large variability of T/ET reported previously in the literature may be related to the length and method of sampling and representativeness of the sites used.

Sites where LAI $<$ 1 correspond to semi-arid areas with patchy vegetation. Measurement and modelling of evaporation and transpiration fluxes in such locations, although extremely important, remains challenging. We are confident that the model results presented in this study are unlikely to be considerably biased when LAI $<$ 1, because, in order to sustain productivity in semi-arid regions (Sala *et al* 1988, Cleland *et al* 2013, Biederman *et al* 2017), long-term transpiration cannot be a small fraction of ET. Otherwise water use efficiency would need to be extremely high in these ecosystems, which is not supported by current estimates (Beer *et al* 2009, Tang *et al* 2014). The bias is most likely to emerge from measurement uncertainties. Observation-based transpiration and evapotranspiration estimates are typically carried out for short periods during the growing season or inferred with indirect methods. Misrepresentation of vegetation transpiration response following major (but infrequent) rainfall events would likely bias and lower the average T/ET ratio.

4. Conclusions

By jointly analysing process-based model simulation results and observations, for the present climate, T/ET for natural and undisturbed ecosystems is well constrained at the global scale ~70 $\pm$ 9% (mean $\pm$ one standard deviation). The biotic (transpiration) and abiotic (soil evaporation, evaporation from interception) components of ET are strongly influenced in a complementary manner by climate (primarily by rainfall amount and structure), and vegetation attributes (primarily LAI). The reason for the constancy in T/ET across a wide range of ecosystems analysed in this study is that vegetation is adapted to local climate and thus produces leaf area that covaries with rainfall properties in a manner that constrains T/ET. This constraint originates from the compensation between different components of ET, which can be limited by either water or energy supply. For conditions where vegetation is not in equilibrium with local climate (e.g. agricultural land, irrigated lands or degraded pastures), the values of T/ET are substantially different. Ecosystems with special hydrological regimes (boreal peatlands, wetlands, groundwater fed ecosystems) were not analysed in this study and may also result to different values of T/ET. Our analysis revealed that predicted climate change scenarios can only marginally modify T/ET leading to the conclusion that T/ET

will remain a well constrained quantity also in the future.

Acknowledgments

Publically available data for this study were obtained by the Fluxnet project (https://daac.ornl.gov/cgi-bin/dataset_lister.pl?p=9), the climatic research unit of the University of East Anglia (http://cru.uea.ac.uk/), the GLASS project (http://glcf.umd.edu/data/lai/). We acknowledge the PIs of the rainfall manipulation and long-term sites that shared their data. CP acknowledges the support of the Swiss National Science Foundation (Grant P300P2_174477).

ORCID iDs

Athanasios Paschalis https://orcid.org/0000-0003-4833-9962

References

Araújo A C 2002 Comparative measurements of carbon dioxide fluxes from two nearby towers in a central Amazonian rainforest: The Manaus LBA site *J. Geophys. Res.* **107** 8090

Baldocchi D D, Xu L and Kiang N 2004 How plant functional-type, weather, seasonal drought, and soil physical properties alter water and energy fluxes of an oak–grass savanna and an annual grassland *Agric. Forest Meteorol.* **123** 13–39

Beer C, Ciais P, Reichstein M, Baldocchi D, Law B E, Papale D and Wohlfahrt G 2009 Temporal and among-site variability of inherent water use efficiency at the ecosystem level *Glob. Biogeochem. Cycles* **23**

Berkelhammer M, Noone D C, Wong T E, Burns S P, Knowles J F, Kaushik A and Williams M W 2016 Convergent approaches to determine an ecosystem's transpiration fraction *Glob. Biogeochem. Cycles* **30** 933–51

Biederman J A, Scott R L, Bell T W, Bowling D R, Dore S, Garatuza-Payan J and Goulden M L 2017 CO_2 exchange and evapotranspiration across dryland ecosystems of southwestern North America *Glob. Change Biol.* **23** 4204–21

Buckley T N and Mott K A 2013 Modelling stomatal conductance in response to environmental factors *Plant Cell Environ.* **36** 1691–9

Cavanaugh M L, Kurc S A and Scott R L 2011 Evapotranspiration partitioning in semiarid shrubland ecosystems: a two-site evaluation of soil moisture control on transpiration *Ecohydrology* **4** 671–81

Caylor K K, Scanlon T M and Rodríguez-Iturbe I 2009 Ecohydrological optimization of pattern and processes in water-limited ecosystems: a trade-off-based hypothesis *Water Resour. Res.* **45**

Choudhury B J and DiGirolamo N E 1998 A biophysical process-based estimate of global land surface evaporation using satellite and ancillary data I. Model description and comparison with observations *J. Hydrol.* **205** 164–85

Cleland E E, Collins S L, Dickson T L, Farrer E C, Gross K L, Gherardi L A and Suding K N 2013 Sensitivity of grassland plant community composition to spatial versus temporal variation in precipitation *Ecology* **94** 1687–96

Coenders-Gerrits A M J, van der Ent R J, Bogaard T A, Wang-Erlandsson L, Hrachowitz M and Savenije H H G 2014 Uncertainties in transpiration estimates *Nature* **506** E1–2

Curtis P S, Vogel C S, Gough C M, Schmid H P, Su H-B and Bovard B D 2005 Respiratory carbon losses and the carbon-use efficiency of a northern hardwood forest, 1999–2003 *New Phytologist* **167** 437–56

Fatichi S, Ivanov V Y and Caporali E 2012a A mechanistic ecohydrological model to investigate complex interactions in cold and warm water-controlled environments: I. Theoretical framework and plot-scale analysis *J. Adv. Model. Earth Syst.* **4**

Fatichi S, Ivanov V Y and Caporali E 2012b A mechanistic ecohydrological model to investigate complex interactions in cold and warm water-controlled environments: II. Spatiotemporal analyses *J. Adv. Model. Earth Syst.* **4**

Fatichi S, Leuzinger S, Paschalis A, Langley J A, Donnellan Barraclough A and Hovenden M J 2016a Partitioning direct and indirect effects reveals the response of water-limited ecosystems to elevated CO_2 *Proc. Natl Acad. Sci.* **113** 12757–62

Fatichi S and Pappas C 2017 Constrained variability of modeled T : ET ratio across biomes *Geophys. Res. Lett.* **44** 6795–803

Fatichi S, Pappas C and Ivanov V Y 2016b Modeling plant-water interactions: an ecohydrological overview from the cell to the global scale *Wiley Interdiscip. Rev.: Water* **3** 327–68

Fischer E M, Seneviratne S I, Vidale P L, Lüthi D and Schär C 2007 Soil moisture–atmosphere interactions during the 2003 European summer heat wave *J. Clim.* **20** 5081–99

Gash J H C 1979 An analytical model of rainfall interception by forests *Q. J. R. Meteorol. Soc.* **105** 43–55

Gentine P, Holtslag A A M, D'Andrea F and Ek M 2013 Surface and atmospheric controls on the onset of moist convection over land *J. Hydrometeorol.* **14** 1443–62

Good S P, Noone D and Bowen G 2015 Hydrologic connectivity constrains partitioning of global terrestrial water fluxes *Science* **349** 175–7

Hardiman B S, Bohrer G, Gough C M, Vogel C S and Curtis P S 2011 The role of canopy structural complexity in wood net primary production of a maturing northern deciduous forest *Ecology* **92** 1818–27

Harris I, Jones P D, Osborn T J and Lister D H 2014 Updated high-resolution grids of monthly climatic observations-the CRU TS3.10 Dataset *Int. J. Climatol.* **34** 623–42

Houze R A 2004 Mesoscale convective systems *Rev. Geophys.* **42** RG4003

Jasechko S, Sharp Z D, Gibson J J, Birks S J, Yi Y and Fawcett P J 2013 Terrestrial water fluxes dominated by transpiration *Nature* **496** 347–50

Katul G G, Oren R, Manzoni S, Higgins C and Parlange M B 2012 Evapotranspiration: a process driving mass transport and energy exchange in the soil-plant-atmosphere-climate system *Rev. Geophys.* **50** 1–25

Keenan T, Sabate S and Gracia C 2010 Soil water stress and coupled photosynthesis–conductance models: bridging the gap between conflicting reports on the relative roles of stomatal, mesophyll conductance and biochemical limitations to photosynthesis *Agric. Forest Meteorol.* **150** 443–53

Knutti R and Sedláček J 2012 Robustness and uncertainties in the new CMIP5 climate model projections *Nat. Clim. Change* **3** 369–73

Kool D, Agam N, Lazarovitch N, Heitman J L, Sauer T J and Ben-Gal A 2014 A review of approaches for evapotranspiration partitioning *Agric. Forest Meteorol.* **184** 56–70

Lorenz R, Jaeger E B and Seneviratne S I 2010 Persistence of heat waves and its link to soil moisture memory *Geophys. Res. Lett.* **37** 1–5

Manoli G, Domec J C, Novick K, Oishi A C, Noormets A, Marani M and Katul G G 2016 Soil-plant-atmosphere conditions regulating convective cloud formation above southeastern US pine plantations *Glob. Change Biol.* **22** 2238–54

Manoli G, Meijide A, Huth N, Knohl A, Kosugi Y, Burlando P, Ghazoul J and Fatichi S 2018 Ecohydrological changes after tropical forest conversion to oil palm *Environ. Res. Lett.* **13** 064035

Manzoni S, Vico G, Katul G, Palmroth S and Porporato A 2014 Optimal plant water-use strategies under stochastic rainfall *Water Resour. Res.* **50** 5379–94

Mastrotheodoros T, Pappas C, Molnar P, Burlando P, Keenan T F, Gentine P and Fatichi S 2017 Linking plant functional trait plasticity and the large increase in forest water use efficiency *J. Geophys. Res.: Biogeosci.* **122** 2393–408

Mccarthy H R, Oren R, Finzi A C, Ellsworth D S, Lim H-S, Johnsen K H and Millar B 2007 Temporal dynamics and spatial variability in the enhancement of canopy leaf area under elevated atmospheric CO_2 *Glob. Change Biol.* **13** 2479–97

Mendelsohn R, Morrison W, Schlesinger M E and Andronova N G 2000 Country-specific market impacts of climate change *Clim. Change* **45** 553–69

Oki T and Kanae S 2006 Global hydrological cycles and world water resources *Science* **313** 1068–72

Pappas C, Fatichi S and Burlando P 2016 Modeling terrestrial carbon and water dynamics across climatic gradients: does plant trait diversity matter? *New Phytologist* **209** 137–51

Paschalis A, Fatichi S, Katul G G and Ivanov V Y 2015 Cross-scale impact of climate temporal variability on ecosystem water and carbon fluxes *J. Geophys. Res.: Biogeosci.* **120** 1716–40

Paschalis A, Katul G G, Fatichi S, Manoli G and Molnar P 2016 Matching ecohydrological processes and scales of banded vegetation patterns in semiarid catchments *Water Resour. Res.* **52**

Paschalis A, Katul G G, Fatichi S, Palmroth S and Way D 2017 On the variability of the ecosystem response to elevated atmospheric CO_2 across spatial and temporal scales at the Duke Forest FACE experiment *Agric. Forest Meteorol.* **232** 367–83

Poorter H, Niinemets Ü, Poorter L, Wright I J and Villar R 2009 Causes and consequences of variation in leaf mass per area (LMA): a meta-analysis *New Phytologist* **182** 565–88

Reich P B, Ellsworth D S and Walters M B 1998 Leaf structure (specific leaf area) modulates photosynthesis-nitrogen relations: evidence from within and across species and functional groups *Funct. Ecol.* **12** 948–58

Sala O E, Parton W, Joyce L A and Lauenroth W K 1988 Primary production of the central grassland region of the United States *Ecology* **69** 40–5

Schlesinger W H and Jasechko S 2014 Transpiration in the global water cycle *Agric. Forest Meteorol.* **190** 115–7

Schmidhuber J and Tubiello F N 2007 Global food security under climate change *Proc. Natl Acad. Sci.* **104** 19703–8

Scott R L, Biederman J A, Hamerlynck E P and Barron-Gafford G A 2015 The carbon balance pivot point of southwestern U.S. semiarid ecosystems: insights from the 21st century drought *J. Geophys. Res.: Biogeosci.* **120** 2612–24

Seneviratne S I, Corti T, Davin E L, Hirschi M, Jaeger E B, Lehner I and Teuling A J 2010 Investigating soil moisture-climate interactions in a changing climate: a review *Earth-Sci. Rev.* **99** 125–61

Suni T, Rinne J, Reissell A, Altimir N, Keronen P, Rannik U and Vesala T 2003 Long-term measurements of surface fluxes above a scots pine forest in Hyytiala, southern Finland, 1996-2001 *Boreal Environ. Res.* **8** 287–301

Tang X, Li H, Desai A R, Nagy Z, Luo J, Kolb T E and Ammann C 2014 How is water-use efficiency of terrestrial ecosystems distributed and changing on Earth? *Sci. Rep.* **4** 1–11

Wang K and Dickinson R E 2012 A review of global terrestrial evapotranspiration: observation, modeling, climatology, and climatic variability *Rev. Geophys.* **50** 1–54

Wang L, Good S P and Caylor K K 2014 Global synthesis of vegetation control on evapotranspiration partitioning *Geophys. Res. Lett.* **41** 6753–7

Warren R K, Pappas C, Helbig M, Chasmer L E, Berg A A, Baltzer J L and Sonnentag O 2018 Minor contribution of overstorey transpiration to landscape evapotranspiration in boreal permafrost peatlands *Ecohydrology* **11** e1975

Wei Z, Yoshimura K, Wang L, Miralles D G, Jasechko S and Lee X 2017 Revisiting the contribution of transpiration to global terrestrial evapotranspiration *Geophys. Res. Lett.* **44** 2792–801

Wild M, Folini D, Hakuba M Z, Schär C, Seneviratne S I, Kato S and König-Langlo G 2015 The energy balance over land and oceans: an assessment based on direct observations and CMIP5 climate models *Clim. Dyn.* **44** 3393–429

Xiao Z, Liang S, Wang J, Chen P, Yin X, Zhang L and Song J 2014 Use of general regression neural networks for generating the GLASS leaf area index product from time-series MODIS surface reflectance *IEEE Trans. Geosci. Remote Sens.* **52** 209–23

Zhang Y, Peña-Arancibia J L, McVicar T R, Chiew F H S, Vaze J, Liu C and Pan M 2016 Multi-decadal trends in global terrestrial evapotranspiration and its components *Sci. Rep.* **6** 19124

Zhou S, Yu B, Zhang Y, Huang Y and Wang G 2016 Partitioning evapotranspiration based on the concept of underlying water use efficiency *Water Resour. Res.* **52** 1160–75